View metadata, citation and similar papers at core.ac.uk
brought to you by CORE
provided by DigitalCommons@The Texas Medical Center

Natriuretic Peptides and Nitric Oxide Stimulate cGMP Synthesis in Different Cellular Compartments

Leslie A. Piggott,[1] Kathryn A. Hassell,[3] Zuzana Berkova,[3] Andrew P. Morris,[1,3] Michael Silberbach,[2] and Thomas C. Rich[1,3]

[1]Program in Cell and Regulatory Biology, The University of Texas Graduate School of Biomedical Sciences at Houston, Houston, TX 77225
[2]Department of Pediatrics and the Heart Research Center, Oregon Health and Science University, Portland, OR 97239
[3]Department of Integrative Biology and Pharmacology, University of Texas Health Science Center at Houston, Houston, TX 77030

Cyclic nucleotide-gated (CNG) channels are a family of ion channels activated by the binding of cyclic nucleotides. Endogenous channels have been used to measure cyclic nucleotide signals in photoreceptor outer segments and olfactory cilia for decades. Here we have investigated the subcellular localization of cGMP signals by monitoring CNG channel activity in response to agonists that activate either particulate or soluble guanylyl cyclase. CNG channels were heterologously expressed in either human embryonic kidney (HEK)-293 cells that stably overexpress a particulate guanylyl cyclase (HEK-NPRA cells), or cultured vascular smooth muscle cells (VSMCs). Atrial natriuretic peptide (ANP) was used to activate the particulate guanylyl cyclase and the nitric oxide donor S-nitroso-n-acetylpenicillamine (SNAP) was used to activate the soluble guanylyl cyclase. CNG channel activity was monitored by measuring Ca^{2+} or Mn^{2+} influx through the channels using the fluorescent dye, fura-2. We found that in HEK-NPRA cells, ANP-induced increases in cGMP levels activated CNG channels in a dose-dependent manner (0.05–10 nM), whereas SNAP (0.01–100 μM) induced increases in cGMP levels triggered little or no activation of CNG channels ($P < 0.01$). After pretreatment with 100 μM 3-isobutyl-1-methylxanthine (IBMX), a nonspecific phosphodiesterase inhibitor, ANP-induced Mn^{2+} influx through CNG channels was significantly enhanced, while SNAP-induced Mn^{2+} influx remained small. In contrast, we found that in the presence of IBMX, both 1 nM ANP and 100 μM SNAP triggered similar increases in total cGMP levels. We next sought to determine if cGMP signals are compartmentalized in VSMCs, which endogenously express particulate and soluble guanylyl cyclase. We found that 10 nM ANP induced activation of CNG channels more readily than 100 μM SNAP; whereas 100 μM SNAP triggered higher levels of total cellular cGMP accumulation. These results suggest that cGMP signals are spatially segregated within cells, and that the functional compartmentalization of cGMP signals may underlie the unique actions of ANP and nitric oxide.

The Journal of General Physiology

INTRODUCTION

Natriuretic peptide receptors and soluble guanylyl cyclase (sGC) are activated by the binding of natriuretic peptides and nitric oxide (NO), respectively. In turn, these enzymes synthesize cGMP, the second messenger that is critically important to the maintenance of vascular tone, cardiac contractility, cardioprotective responses to ischemia, and cellular proliferation (Hartzell and Fischmeister, 1986; Ruskoaho et al., 1987; Waldman and Murad, 1988; Furchgott and Vanhoutte, 1989; Schulz et al., 1989; Ignarro et al., 1999; Hanafy et al., 2001; Rybalkin et al., 2003; Kuhn, 2004; Baxter, 2004; D'Souza et al., 2004; Costa et al., 2005).

Increases in intracellular cGMP levels activate protein kinase G (PKG), which phosphorylates many downstream targets, including phospholamban (Li et al., 1996; Wollert et al., 2003; Zhang et al., 2005b) and mitochondrial K_{ATP} channels (Costa et al., 2005). cGMP also regulates phosphodiesterase activity in a type-specific manner, stimulating phosphodiesterase (PDE) types 2 and 5 while inhibiting PDE type 3 (Martins et al., 1982; Hartzell and Fischmeister, 1986; Beavo, 1995; Wyatt et al., 1998; Palmer and Maurice, 2000; Abi-Gerges et al., 2002). There is also evidence suggesting that elevated levels of cAMP or cGMP increase expression of PDE, including specific isoforms of PDE type 5 (Giordano et al., 1999; Kotera et al., 1999; Lin et al., 2001). Importantly, recent studies have shown that increases in cGMP levels triggered by natriuretic peptides and NO donors lead to regulation of different cellular targets (Zolle et al., 2000; Rho et al., 2002; Zhang et al., 2005a). Similarly, exposure of HEK-NPRA cells to atrial natriuretic peptide (ANP) triggers the redistribution of PKG to the plasma membrane, but exposure to NO donors does not (Airhart et al., 2003). What remains unclear are the

Correspondence to Thomas C. Rich: trich@jaguar1.usouthal.edu

The online version of this article contains supplemental material.

Abbreviations used in this paper: ANP, atrial natriuretic peptide; CNG, cyclic nucleotide-gated; HEK, human embryonic kidney; IBMX, 3-isobutyl-1-methylxanthine; NO, nitric oxide; NPRA, natriuretic peptide receptor A; PDE, phosphodiesterase; sGC, soluble guanylyl cyclase; SNAP, S-nitroso-n-acetylpenicillamine; VSMC, vascular smooth muscle cell.

mechanisms by which ANP and NO donors differentially regulate cellular processes.

One intriguing possibility is that cGMP signals are compartmentalized, or localized, to distinct regions of the cell. We have previously presented several lines of evidence suggesting that cAMP signals are compartmentalized, and that hindered diffusion, buffering, and PDE activity play critical roles in generating spatially and temporally distinct cAMP signals (Rich et al., 2000, 2001a; Rich and Karpen, 2002). These conclusions were based on four observations obtained using cyclic nucleotide-gated (CNG) channels as real-time sensors for cAMP signals: (1) the cAMP concentration near the CNG channels was ~10-fold higher than total cellular concentration, (2) cAMP signals measured using CNG channels were resistant to washout of the cytosol with the whole cell patch pipette, (3) the wash-in of cAMP from the patch pipette to CNG channels was slow, and (4) kinetically distinct cAMP signals coexist within the same cells. Based upon these results we developed a compartmental model to describe the spatial segregation of cyclic nucleotide signals within cells. One prediction of this model is that activation of particulate or soluble cyclase would give rise to spatially distinct cyclic nucleotide signals. Details of the model and simulations used for this prediction are included in the online supplemental material (available at http://www.jgp.org/cgi/content/full/jgp.200509403/DC1).

In the present study we test this prediction by examining the efficacy with which CNG channels are activated by cGMP produced in response to stimulation of particulate or soluble guanylyl cyclase (pGC or sGC). We found that in both human embryonic kidney (HEK)-293 cells stably overexpressing natriuretic peptide receptor A (NPRA) (HEK-NPRA cells) and cultured vascular smooth muscle cells (VSMCs), stimulation with 1 or 10 nM ANP activated CNG channels far more readily than 100 μM S-nitroso-N-acetylpenicillamine (SNAP), an NO donor, even when cells were pretreated with 3-isobutyl-1-methylxanthine (IBMX), a nonspecific PDE inhibitor. We measured total cGMP levels in the same cells using enzyme immunoassays and found that following pretreatment with IBMX, there was either no significant difference between ANP and SNAP-induced total cGMP accumulation (HEK-NPRA cells), or significantly higher SNAP-induced total cGMP accumulation (VSMCs). These data strongly suggest that cGMP signals are functionally localized to different subcellular compartments, and also indicate that PDE activity may not be solely responsible for the localization of cGMP signals over a 5-min timescale.

MATERIALS AND METHODS

Cell Culture and Channel Expression

HEK-NPRA cells (Airhart et al., 2003) were maintained in Dulbecco's modified Eagle's medium (DMEM) containing 10% (vol/vol) FBS, 400 μg/ml G418, 2 g/liter sodium bicarbonate, 100 μg/ml streptomycin, and 100 U/ml penicillin at 37°C in a humidified atmosphere of 95% air, 5% CO_2. Cells were plated at 20–30% confluence, grown for 48 h, and then infected with a previously described adenovirus encoding the CNGA2 subunit, MOI = 10 pfu/cell (Fagan et al., 1999). 6 h after infection, cells were serum starved in media containing 1% FBS and 1 mM hydroxyurea to inhibit viral replication. 24 h after infection, cells were detached with PBS containing 0.03% EDTA, resuspended in serum-free media buffered with 20 mM HEPES, pH 7.2, and assayed within 6 h.

Rat vascular smooth muscle cells were isolated and maintained as described previously (Ostrom et al., 2002; Zhang et al., 2003). In brief, adult male Sprague-Dawley rats were killed with intraperitoneal pentobarbital sodium, the thoracic arteries were dissected, and endothelial layers were removed. The aortas were minced and digested with collagenase type I and elastase type V at 37°C. Cells were plated and maintained in DMEM containing 10% (vol/vol) FBS, 100 μg/ml streptomycin, and 100 U/ml penicillin, in a humidified atmosphere of 95% air, 5% CO_2. Passages 4–10 were used for the experiments described here; under our culture conditions cells from these passages maintained a contractile phenotype. Cells were plated at 50% confluence onto laminin-coated coverslips and infected with adenovirus encoding the CNGA2 subunit, MOI = 100 pfu/cell, as described in Rich and Karpen (2005). 6 h after infection, cells were washed with fresh media, and 48 h after infection, cells were assayed as described below.

Monitoring CNG Channel Activation in Cell Populations

To monitor the activation of CNG channels in cell populations, we measured Ca^{2+} or Mn^{2+} influx through the channels. In this assay, increases in intracellular cGMP (e.g., triggered by exposing cells to ANP) activate CNG channels, allowing the influx of cations, including Ca^{2+} and Mn^{2+}, through the channels. Intracellular Ca^{2+} and Mn^{2+} concentrations were monitored using the fluorescent dye fura-2 (Molecular Probes). Details of the experimental procedure were described previously (Rich et al., 2001b). In brief, cells were loaded with 8 μM fura-2/AM (3×10^6 cells/ml buffer). After 45 min, cells were washed three times and resuspended in an extracellular buffer containing (in mM) 145 NaCl, 4 KCl, 10 HEPES, 10 D-glucose, 1 $MgCl_2$, 1 $CaCl_2$, pH 7.35. In some experiments we monitored Mn^{2+} influx through CNG channels by measuring Mn^{2+}quench of fura-2 at an excitation wavelength of 360 nm (the isosbestic point for fura-2 at different Ca^{2+} concentrations). In these experiments, cells were pelleted and resuspended in the extracellular buffer with 5 μM $MnCl_2$ immediately preceding the start of the assay. Data were acquired using either PTI DeltaScan or QuantaMaster spectrofluorimeters. Fluorescence was monitored at excitation wavelengths of 360 and 380 nm and an emission wavelength of 510 nm. Data were sampled at either 5 or 0.5 Hz, filtered at 1 or 0.2 Hz, and expressed relative to the prestimulus fluorescence (F_0) to correct for variations in dye concentration, and to allow for comparison of results on different batches of cells. To quantify the data, lines were fit to the slopes of the change in fluorescence over time (see Fig. 7). Compiled data are represented as the mean ± SEM, and significance was assessed using the Student's paired *t* test. Additions were made from stock solutions (with final vehicle concentrations <0.2%) to a stirred cuvette (mixing time of ~5 s); thus, after addition all agents were present throughout the assay. ANP, IBMX, and SNAP were purchased from Calbiochem. Unless otherwise stated, all other chemicals were purchased from Sigma-Aldrich. Data are representative of at least four experiments.

Monitoring CNG channel activation in single cells

48 h after infection, VSMCs were loaded with 8 μM fura2-AM for 90 min in the extracellular buffer described above. Coverslips

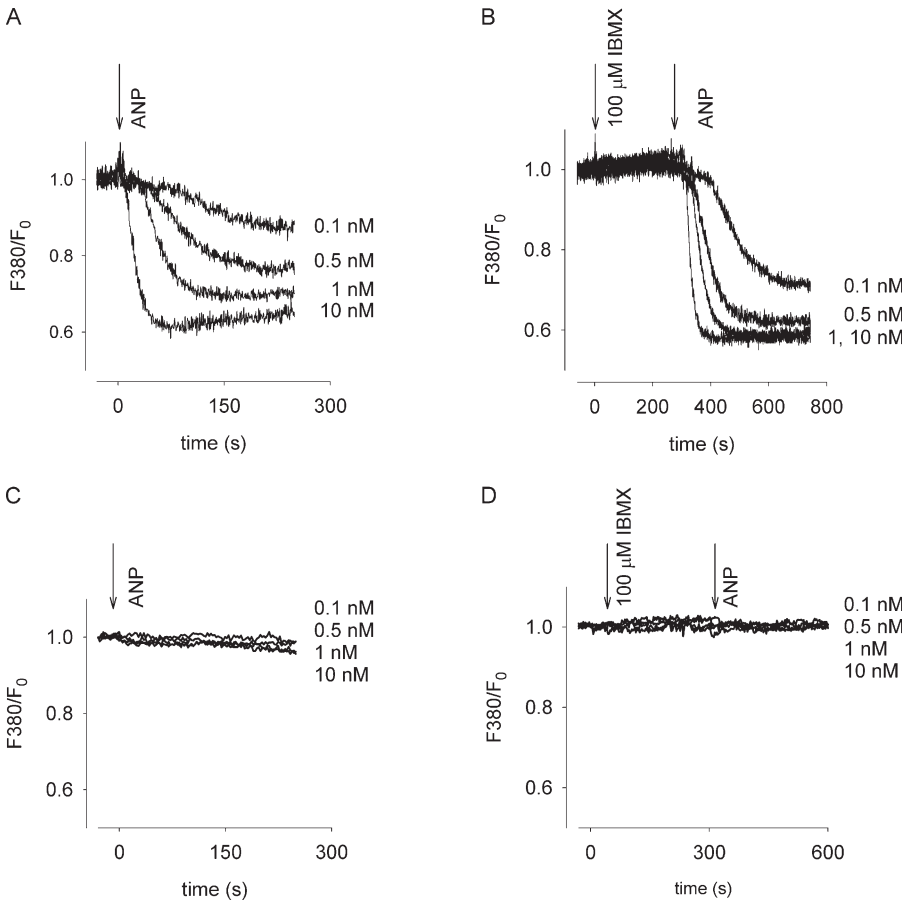

Figure 1. ANP-induced Ca^{2+} responses in CNG channel-expressing HEK-NPRA cells. (A) Plasma membrane–localized cGMP signals were detected in cell populations using Ca^{2+} influx through CNG channels composed of CNGA2 subunits. Ca^{2+} influx caused a decrease in fluorescence monitored at an excitation wavelength of 380 nm (F/F_0). ANP was added at the indicated concentrations at 0 s (arrow), and caused a dose-dependent rise in intracellular Ca^{2+}. (B) In the presence of the PDE inhibitor IBMX (100 μM, added at 0 s), the ANP-induced Ca^{2+} responses were significantly potentiated. (C and D) Addition of ANP alone (C) or after pretreatment with IBMX (D) did not trigger Ca^{2+} responses in control cells (cells not expressing CNG channels).

were then mounted onto measurement chambers and continuously perfused with buffer. Cells were assayed at room temperature in a buffer containing (in mM) 145 NaCl, 4 KCl, 10 HEPES, 10 D-glucose, 1 $MgCl_2$, 0.1 $CaCl_2$, 0.005 $MnCl_2$, 0.001 nimodipine, pH 7.35. To monitor CNG channel activation we measured Mn^{2+} influx at an excitation wavelength of 360 nm and an emission wavelength of 510 nm using a high-resolution camera system. Cellular fluorescence was defined by windows placed around individual cells, images and total intensities from each cell were acquired, and background fluorescence was corrected on-line. Data were analyzed as described above.

Measurement of Total cGMP and cAMP Levels

Total cGMP and cAMP levels in HEK-NPRA and vascular smooth muscle cells were measured using either cGMP or cAMP binding assays (EIA Biotrak System, Amersham and Direct cAMP, Assay Designs). In brief, experiments were conducted either on cells attached to 12-well plates, or to cells in suspension, as indicated. For the experiments conducted on cells in suspension, CNG channel activity (Mn^{2+} influx) was first monitored as described above. Immediately following these measurements, cGMP accumulation was terminated by addition of HCl (0.1 N, final concentration). Samples were neutralized with 1 N NaOH. In both sets of experiments cGMP accumulation was initiated using SNAP or ANP, and PDE activity was inhibited using IBMX as indicated. Sample cGMP and cAMP contents were calculated from standard curves. Under our experimental conditions, stimulation with ANP or SNAP and IBMX did not trigger significant cAMP accumulation. To ensure that no significant extrusion of cGMP occurred we measured both cellular and extruded cGMP from HEK-NPRA cells attached to 60-mm dishes. We found that under these experimental conditions <1% of the total cGMP was extruded from HEK-NPRA cells during a 5-min stimulation with 1 nM ANP or 100 μM SNAP. Data are represented as the mean ± SEM, performed in triplicate. Significance was assessed using the Student's paired *t* test.

Online Supplemental Material

The online supplemental material (Figs. S1–S3, available at http://www.jgp.org/cgi/content/full/jgp.200509403/DC1) presents a mathematical model that predicts activation of either particulate or soluble guanylyl cyclase will give rise to spatially segregated cGMP signals.

RESULTS

CNG Channels Are Readily Activated by ANP-induced cGMP Signals

We first wanted to determine if CNG channels would respond to increases in intracellular cGMP levels triggered by activation of NPRA. CNG channels composed of four CNGA2 subunits have a $K_{1/2}$ for cGMP of ~2 μM and $K_{1/2}$ for cAMP of ~40 μM (Dhallan et al., 1990). We have found that functional CNG channels were expressed in >90% of HEK-293 cells when CNGA2 subunits were expressed using adenovirus constructs. These results were based on direct measurements of CNG channel activity made using excised patch or whole cell patch clamp configurations (Rich et al., 2000;

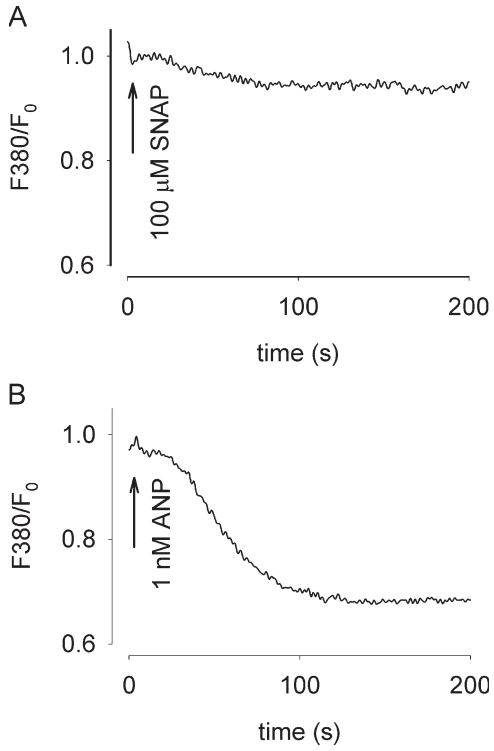

Figure 2. ANP triggered Ca^{2+} responses more readily than SNAP in CNG channel-expressing cells. (A) 100 μM SNAP triggered little or no response in CNG channel-expressing cells. (B) 1 nM ANP (added at 0 s, arrow) induces a large rise in Ca^{2+} in the same batch of CNG channel-expressing cells used in A. ANP and SNAP triggered little or no Ca^{2+} response in control cells (not depicted).

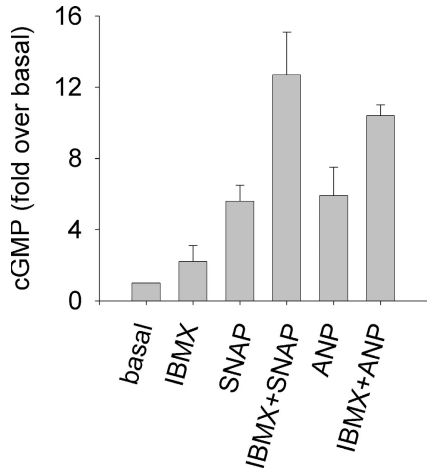

Figure 3. Both ANP and SNAP trigger significant increases in intracellular cGMP. Intracellular cGMP was measured in HEK-NPRA cells as described in Materials and Methods. Cells were treated for 5 min with 1 nM ANP, 100 μM SNAP, or pretreated with 100 μM IBMX for 5 min followed by 5 min with 1 nM ANP or 100 μM SNAP, as indicated. It is apparent that both ANP and SNAP trigger significant accumulation of intracellular cGMP, and that cGMP accumulation is potentiated by exposure to IBMX. Less than 1% of the total cGMP was extruded under these conditions (not depicted). These data are the average ± SEM of three experiments done in triplicate.

Rich et al., 2001a,b). In this study, activation of CNG channels was monitored in populations of HEK-NPRA cells by measuring changes in intracellular Ca^{2+} levels using fura-2 (Frings et al., 1995; Rich et al., 2001b). The experiments were conducted in cell populations (3×10^6 cells per cuvette) to ensure an appropriate comparison to the enzyme immunoassays for total cGMP levels discussed later. We observed that the addition of increasing concentrations of ANP (0.1–10 nM) led to dose-dependent increases in intracellular Ca^{2+} (Fig. 1 A). Pretreatment of cells with the nonspecific PDE inhibitor IBMX (100 μM, 5 min) significantly enhanced the ANP-induced responses (Fig. 1 B). In control cells (not expressing CNG channels), no ANP-induced responses were observed, even following pretreatment with IBMX (Fig. 1, C and D). In addition, stimulation with ANP or SNAP and IBMX did not trigger significant cAMP accumulation as monitored with enzyme immunoassays or with CNG channels that are insensitive to cGMP (unpublished data). Thus, these data indicate that ANP-induced increases in intracellular cGMP trigger the activation of CNG channels, and subsequent Ca^{2+} responses.

We next tested whether NO-induced activation of sGC and the subsequent increase in intracellular cGMP would trigger Ca^{2+} responses in cells expressing CNG channels. Addition of 100 μM SNAP (a supersaturating concentration), an NO donor, either had no effect or triggered a small change in intracellular Ca^{2+} in CNG channel-expressing cells (Fig. 2 A); yet, ANP induced substantial increases in intracellular Ca^{2+} in the same CNG channel-expressing cells (Fig. 2 B). Little or no response was observed in control cells (unpublished data). These data indicate that cells were responsive to changes in cGMP levels near the plasma membrane. In separate experiments we used enzyme immunoassays to assess total cGMP production in HEK-NPRA cells attached to 12-well plates. We found that in response to a 5-min exposure to 1 nM ANP or 100 μM SNAP, cGMP levels were approximately sixfold greater than basal cGMP levels (Fig. 3). After a 5-min pretreatment with 100 μM IBMX, 5-min exposure to either 1 nM ANP or 100 μM SNAP triggered an ~10-fold increase in cGMP levels. In these experiments <1% of the total cGMP was extruded from cells (unpublished data). Also, stimulation with ANP or SNAP and IBMX did not trigger significant cAMP accumulation (unpublished data). Similar results were found using cells in suspension. Thus, both ANP and SNAP triggered similar levels of total cGMP production.

Observed Responses Were Primarily due to Cation Influx through CNG Channels

We were surprised to find that exposure of cells to 100 μM SNAP did not trigger activation of CNG channels

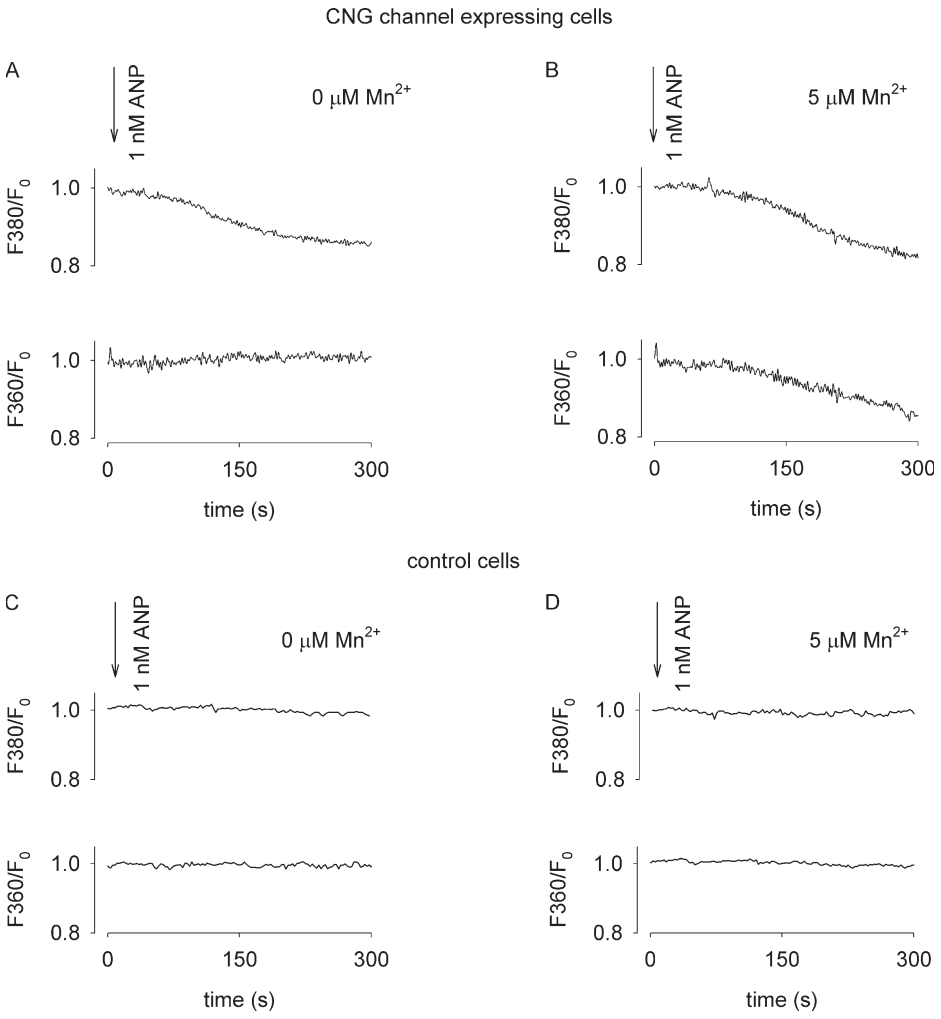

Figure 4. CNG channel activation monitored by measuring Mn^{2+} quench of fura-2 fluorescence. To monitor the activation of CNG channels largely independent of changes in intracellular Ca^{2+} concentration, we measured Mn^{2+} influx through CNG channels (A and B). (A) In the absence of extracellular Mn^{2+}, 1 nM ANP triggered substantial responses at an excitation wavelength of 380 nm but no observable response was observed at an excitation wavelength of 360 nm. (B) In the presence of 5 μM extracellular Mn^{2+}, the response to 1 nM ANP was larger due to both Ca^{2+} binding and Mn^{2+} quench of fura-2 at a wavelength of 380 nm, and substantial quench of the fura-2 signal was observed at a wavelength of 360 nm. (C and D) No response was observed at either wavelength in control cells (not expressing CNG channels) in the absence (C) or presence (D) of 5 μM Mn^{2+}.

because previous studies have provided evidence indicating that NO-generating compounds open CNG channels by S-nitrosylation of a cysteine residue (Broillet, 2000). Thus, we wanted to make certain that ANP had triggered significant activation of CNG channels and that SNAP had not. For example, it seemed possible that exposing cells to ANP or SNAP could have regulated Ca^{2+} handling properties, either augmenting ANP-induced responses (e.g., inhibiting Ca^{2+} pumps or triggering release from intracellular stores), or inhibiting SNAP-induced responses (e.g., stimulating Ca^{2+} pumps). It was also possible that Ca^{2+} influx through CNG channels led to Ca^{2+}-induced Ca^{2+} release (CICR), contributing to the observed Ca^{2+} responses, although we did not observe CICR in our previous studies using CNG channels to monitor cAMP signals in HEK-293 cells (Rich et al., 2001a,b). To ensure that altered Ca^{2+} handling properties of the cells did not contribute to the observed responses, we used a different experimental approach. We found that Mn^{2+} permeates through CNG channels, and were able to monitor Mn^{2+} influx through CNG channels by measuring Mn^{2+} quench of fura-2 at an excitation wavelength of 360 nm (the isosbestic point for fura-2 at different Ca^{2+} concentrations). Given the low extracellular concentrations of Mn^{2+} used in this study (5 μM), and the high Mn^{2+} affinity of fura-2, ~2.8 nM (Kwan and Putney, 1990), it is unlikely that changes in free intracellular Mn^{2+} significantly altered guanylyl cyclase activity. Importantly, this approach allows the measurement of Mn^{2+} influx largely independent of changes in intracellular Ca^{2+} levels. With no Mn^{2+} in the extracellular solution, we observed a large ANP-induced response at an excitation wavelength of 380 nm (Ca^{2+}-sensitive signal) and no response at 360 nm (Ca^{2+}-insensitive signal) (Fig. 4 A). With 5 μM Mn^{2+} in the extracellular solution, we observed ANP-induced responses at both wavelengths (Fig. 4 B). The responses at both excitation frequencies were potentiated following pretreatment with 100 μM IBMX (unpublished data). No responses were observed at either wavelength in control cells (cells not expressing CNG channels, Fig. 4, C and D). These data indicate that ANP-induced increases in intracellular cGMP activate CNG channels, allowing the influx of cations, and

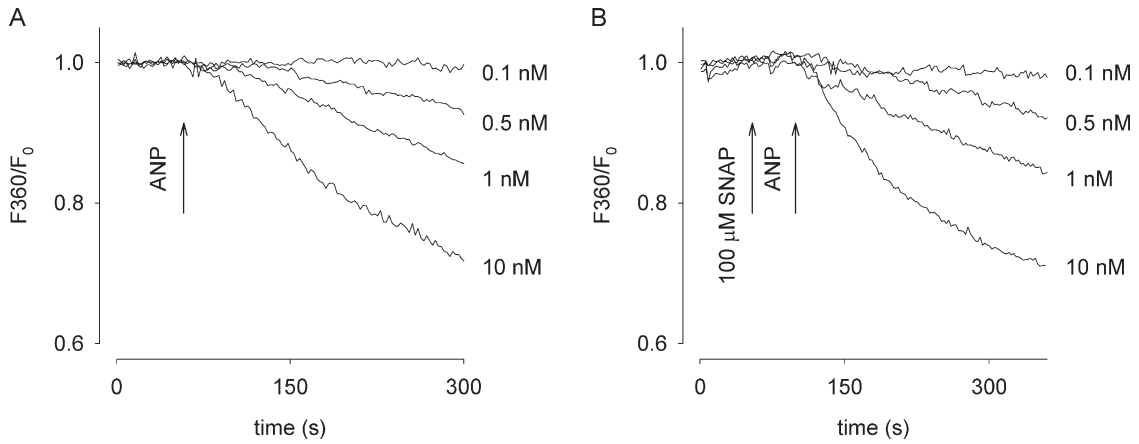

Figure 5. SNAP does not trigger inhibition of CNG channels. We monitored the activation of CNG channels by ANP with or without treating cells for 1 min with 100 μM SNAP. (A) ANP (added at 1 min, arrow) triggered a dose-dependent increase in Mn^{2+} influx though CNG channels. ANP concentrations are indicated at right. (B) Pretreatment with SNAP (added at 1 min, first arrow) did not inhibit ANP (added at 2 min, second arrow)-induced activation of CNG channels, and the dose dependence of channel activation was not altered. ANP concentrations are again indicated at right. These data suggest that the inability of cGMP generated by sGC to activate CNG channels is not due to a SNAP-induced inhibition of CNG channels.

that the primary cause of the ANP-induced increases in intracellular Ca^{2+} is influx though CNG channels.

To ensure that exposure of cells to 100 μM SNAP had not inhibited or desensitized CNG channel activity (either directly or via an unknown cellular mechanism), we monitored Mn^{2+} influx through CNG channels in response to ANP (0.1–10 nM) with and without 1 min pretreatment with 100 μM SNAP (Fig. 5, A and B). The dose dependence, time course, and magnitude of the ANP-induced responses were similar, indicating that after exposure to SNAP, CNG channel activity remained largely intact.

Spatial Segregation of cGMP Signals Produced by Particulate and Soluble Guanylyl Cyclase

To help elucidate whether ANP-induced cGMP signals do indeed activate CNG channels more readily than SNAP-induced signals, we compared the relative activation of CNG channels to total cGMP production in the same cells (see Materials and Methods). We used this approach to ensure that cells were treated in exactly the same manner for each assay (measurement of CNG channel activation and enzyme immunoassay). We observed that addition of 100 μM SNAP did not trigger Mn^{2+} influx whereas 1 nM ANP triggered significant influx (Fig. 6, A and B). In this experiment, pretreatment with 100 μM IBMX significantly increased ANP-induced Mn^{2+} influx, but not the SNAP-induced response (Fig. 6, C and D). 5 min after the addition of either ANP or SNAP we stopped the reactions and subsequently measured total cGMP levels using enzyme immunoassays (Fig. 6 E). Interestingly, following pretreatment with IBMX, similar total amounts of cGMP were produced by addition of ANP or SNAP, although the addition of SNAP was much less effective at activating CNG channels.

We quantified the Mn^{2+} influx data by fitting a line to the slope of the fluorescence quench (Fig. 7 A, inset). This slope is a measure of CNG channel activity. The responses to both 1 nM ANP alone and 100 μM IBMX followed by 1 nM ANP were significantly larger than the response to 100 μM IBMX followed by 100 μM SNAP (Student's paired *t* test, four experiments, Fig. 7 A). In the same four experiments, total cGMP levels triggered by 1 nM ANP alone, 100 μM IBMX followed by 1 nM ANP, and 100 μM IBMX followed by 100 μM SNAP were not statistically different (Fig. 7 B). These data indicate that even in the presence of PDE inhibitors, cGMP signals triggered by SNAP are less effective at activating CNG channels than cGMP signals triggered by ANP.

cGMP Signals Are Spatially Segregated in Vascular Smooth Muscle Cells

While the data presented thus far clearly indicate that cGMP signals are compartmentalized in HEK-NPRA cells, we wanted to determine if cGMP signals are also compartmentalized in a cell type that expresses endogenous particulate and soluble guanylyl cyclase. We chose cultured rat VSMCs because they endogenously express both cyclase types, they are readily cultured so that we could repeat the experiments described above, as well as monitor CNG channel activation in single cells, and cGMP signaling is critically important to their physiology (Waldman and Murad, 1988; Potter et al., 2005). Initially we monitored CNG channel activation by measuring Mn^{2+} influx in populations of VSMCs (3×10^6 cells per cuvette), as described in the Materials and Methods. In these experiments 1 μM nimodipine was added at 0 s to inhibit voltage-gated Ca^{2+} channels. We found that 10 nM ANP triggered the activation of CNG channels, whereas 100 μM SNAP did not (Fig. 8, A and B).

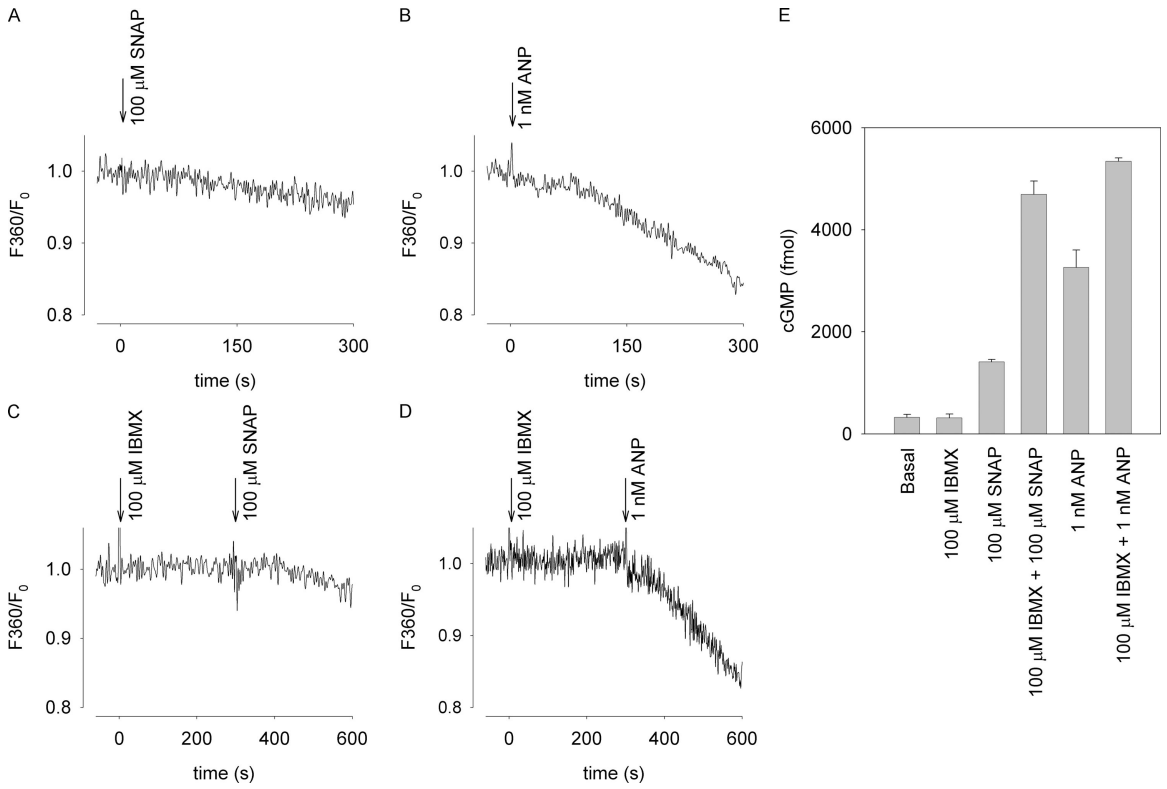

Figure 6. CNG channels functionally colocalize with NPRA. (A) 100 μM SNAP triggered little or no Mn^{2+} influx through CNG channels, whereas (B) 1 nM ANP triggered significant Mn^{2+} influx. (C) Pretreatment with 100 μM IBMX had little effect on SNAP-induced Mn^{2+} influx through CNG channels in this experiment. (D) Pretreatment with 100 μM IBMX significantly potentiated the ANP-induced response. (E) At the end of each experiment (5 min after addition of either SNAP or ANP) the reaction was stopped and the total cGMP was measured using enzyme immunoassays (see Materials and Methods for details). Importantly, similar levels of total cGMP were observed in cells treated with either 100 μM IBMX + 100 μM SNAP or 100 μM IBMX + 1 nM ANP.

Exposure of CNG channel-expressing cells to 100 μM IBMX triggered a small increase in the rate of Mn^{2+} influx (Fig. 8, C and D). Subsequent addition of 10 nM ANP significantly increased the rate of Mn^{2+} influx (Fig. 8 C); subsequent addition of 100 μM SNAP did not (Fig. 8 D). To quantify the level of CNG channel activation, we fit lines to the fluorescence quench as described above. We found that in the absence or presence of 100 μM IBMX, 10 nM ANP triggered significantly more Mn^{2+} influx that 100 μM IBMX and 100 μM SNAP (Student's paired *t* test, four experiments, Fig. 9 A). At the end of each run, we stopped the reaction and measured total cGMP levels using enzyme immunoassays. We found that 100 μM SNAP triggered higher levels of total cGMP accumulation than 10 nM ANP (Student's paired *t* test, four experiments, Fig. 9 B), yet SNAP-induced cGMP accumulation was unable to significantly activate CNG channels in these cells.

To ensure that exposure of VSMCs to 100 μM SNAP had not inhibited or desensitized CNG channel activity, we monitored Mn^{2+} influx through CNG channels in response to 10 nM ANP with and without 5 min pretreatment with 100 μM SNAP. The time course and magnitude of the ANP-induced responses were similar (unpublished data), indicating that after exposure to SNAP, CNG channel activity also remained intact in these cells. Little or no response was observed in control VSMCs (not expressing CNG channels; unpublished data).

We next monitored the activation of CNG channels in single VSMCs (see Materials and Methods). Fig. 10 shows the average response of CNG channel-expressing VSMCs to 10 nM ANP (Fig. 10 A, nine experiments) or 100 μM SNAP (Fig. 10 B, 14 experiments). It is clear that exposure to 10 nM ANP triggered significant activation of CNG channels, whereas exposure to 100 μM SNAP did not. Cells exposed to SNAP were subsequently exposed to 10 nM ANP to ensure that they were expressing CNG channels (unpublished data). Little or no response was observed in control cells (unpublished data). Taken together, these data strongly indicate that cGMP signals are compartmentalized in VSMCs.

DISCUSSION

The goal of this study was to determine if cGMP signals generated by particulate and soluble guanylyl cyclase are equally efficacious in activating CNG channels. To accomplish this we used CNG channels composed of

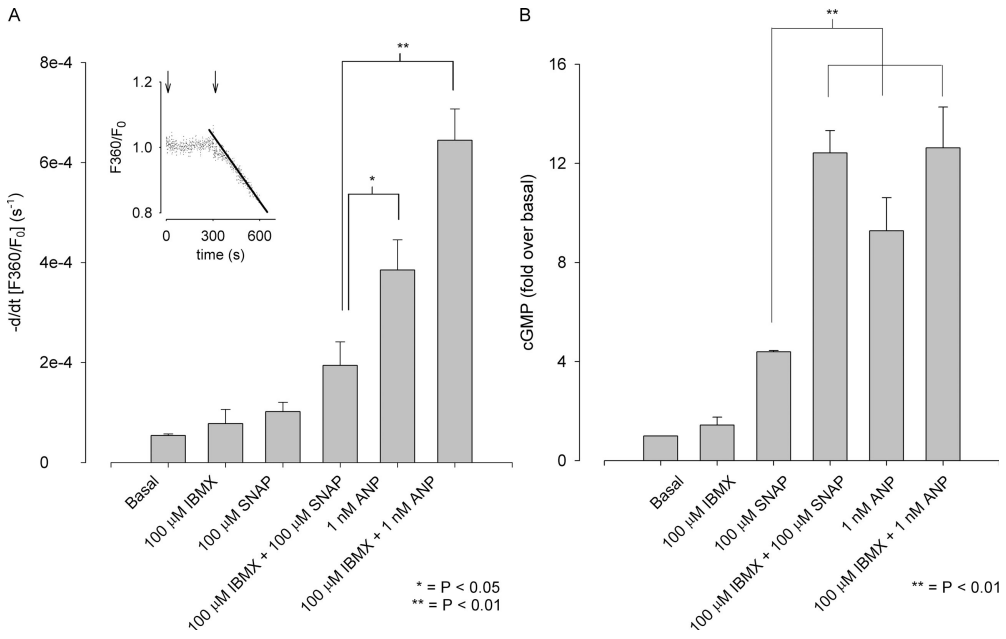

Figure 7. Differential activation of CNG channels by ANP- and SNAP-induced cGMP signals. (A) To quantify the relative levels of CNG channel activation from different experiments, we fit the slope of the fluorescence quench traces with a line using the least squared error criteria (inset). The data clearly indicate that CNG channels are more readily activated in response to either 1 nM ANP or 100 μM IBMX + 1 nM ANP than to 100 μM IBMX + 100 μM SNAP ($P < 0.05$ and 0.01, respectively, four experiments). (B) Averaged total cGMP levels measured using enzyme immunoassays from the same four experiments. The total cGMP levels in response to 100 μM IBMX + 1 nM ANP and 100 μM IBMX + 100 μM SNAP are both similar. These data indicate that CNG channels respond more readily to ANP-induced cGMP signals than to SNAP-induced cGMP signals, and that there is a functional colocalization of CNG channels with NPRA.

adenovirus-expressed rat olfactory α (CNGA2) subunits to monitor cGMP levels near the plasma membrane of HEK-NPRA and cultured vascular smooth muscle cells. We found that under conditions in which SNAP triggered similar (HEK-NPRA cells) or larger (VSMCs) increases in total cGMP levels than ANP, ANP-induced cGMP signals more readily activated CNG channels. These data are consistent with the mathematical model of compartmentalized cGMP signals described in the online supplemental material (available at http://www.jgp.org/cgi/content/full/jgp.200509403/DC1). This model also predicted that cGMP signals would be effectively compartmentalized in the presence of 100 μM IBMX, again consistent with the data presented here. However, residual PDE activity may have contributed to the localization of cGMP responses because IBMX is a competitive inhibitor, and PDE types that are insensitive to IBMX (Soderling et al., 1998) may have been present.

Given the differential effects of PDE inhibitors on near-membrane and total cGMP accumulation (especially in HEK-NPRA cells, see Fig. 7 B), and that the cGMP concentration near the CNG channels was low ($<K_m$ of PDE types 1 or 5, the PDEs responsible for the majority of cGMP hydrolysis in cultured rat VSMCs), it is likely that mechanisms other than residual PDE activity also contributed to the observed segregation of cGMP signals. This indicates that different levels of PDE activity may be responsible for hydrolysis of cGMP signals, and that ANP-induced signals may be somehow protected from the PDE activity that hydrolyzes SNAP-induced signals. Different levels of PDE activity may be due to the presence of distinct PDE types, differential regulation of PDEs, or different PDE concentrations within different subcellular compartments.

What Mechanisms Underlie the Compartmentalization of cGMP Signals?

If PDE activity is not solely responsible for the segregation of cGMP signals, other cellular mechanisms must be involved. Buffering of cAMP and cGMP by protein kinases A and G (PKA and PKG) undoubtedly contributes to the slow spatial spread of cyclic nucleotide signals (Beavo et al., 1974; Rich and Karpen, 2002; Kotera et al., 2003). In particular, subcellular localization of PKA via AKAPs and ligand-dependent association of PKG and NPRA create nonuniform distributions of PKA and PKG within the cells (Gray et al., 1998; Airhart et al., 2003). Structural barriers near the plasma membrane may also contribute to the localization of intracellular signals. For example, there is evidence that ER or SR comes into close apposition to the plasma membrane, and that this may limit the spatial spread of Ca^{2+} and Na^+ in hair cells (Martin and Fuchs, 1992), arterial smooth muscle cells (Arnon et al., 2000), and cardiac myocytes (Bridge et al., 1990; Leblanc and Hume, 1990; Lederer et al., 1990). Such physical barriers would also restrict the spatial spread of larger molecules, including cAMP and cGMP. It is possible that the ER coming in close apposition to the surface membrane contributes to the diffusional restrictions in other cell types (Rich et al., 2000, 2001a). Other structural elements that may also contribute to restricted diffusion are cytoskeleton, dendritic and "mini" spines, and recycled vesicles. Quantitative studies will be required to understand the

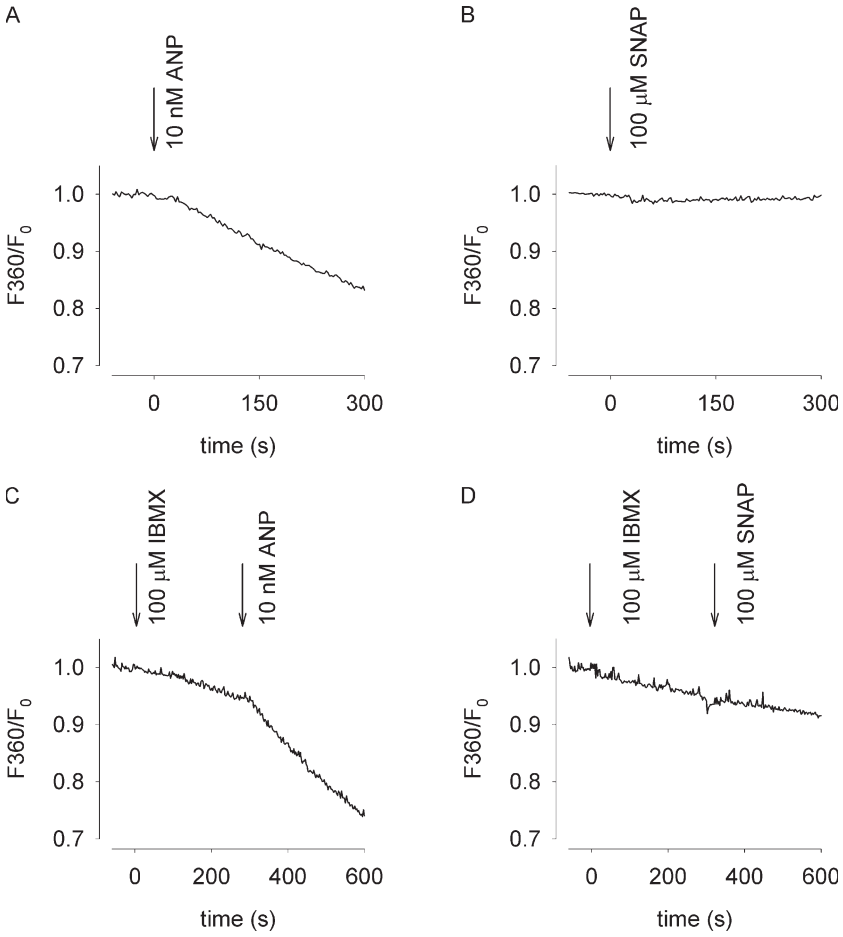

Figure 8. ANP readily induces activation of heterologously expressed CNG channels in populations of cultured VSMCs. CNG channel activation was monitored by measuring Mn^{2+} influx through the channels as described in Materials and Methods. 1 μM nimodipine was added to the extracellular solution at the beginning of the experiment to inhibit endogenous voltage-gated Ca^{2+} channels. (A) Addition of 10 nM ANP (0 s, arrow) triggered activation of CNG channels and influx of Mn^{2+}, whereas addition of 100 μM SNAP (B) did not. (C) Addition of 100 μM IBMX (0 s, first arrow) triggered a small Mn^{2+} influx. Subsequent addition of ANP significantly increased the rate of Mn^{2+} influx (300 s, second arrow). (D) 100 μM IBMX (0 s, first arrow) again triggered a small increase in the rate of Mn^{2+} influx. Subsequent addition of 100 μM SNAP did not further increase the Mn^{2+} influx rate. Subsequent addition of ANP triggered large increases in Mn^{2+} influx (not depicted). These data are summarized in Fig. 9. No responses were observed in control cells (cells not expressing CNG channels, not depicted).

extent to which buffering, PDE activity, and structural barriers contribute to localized signals.

Our previous work demonstrates that two-dimensional colocalization within the plasma membrane is not sufficient for the localized activation of CNG channels by adenylyl or guanylyl cyclase (Rich et al., 2000). However, both cyclase and CNG channels must be present within a given compartment for localized signaling to occur. The results presented here indicate that CNG channels colocalize with particulate guanylyl cyclase

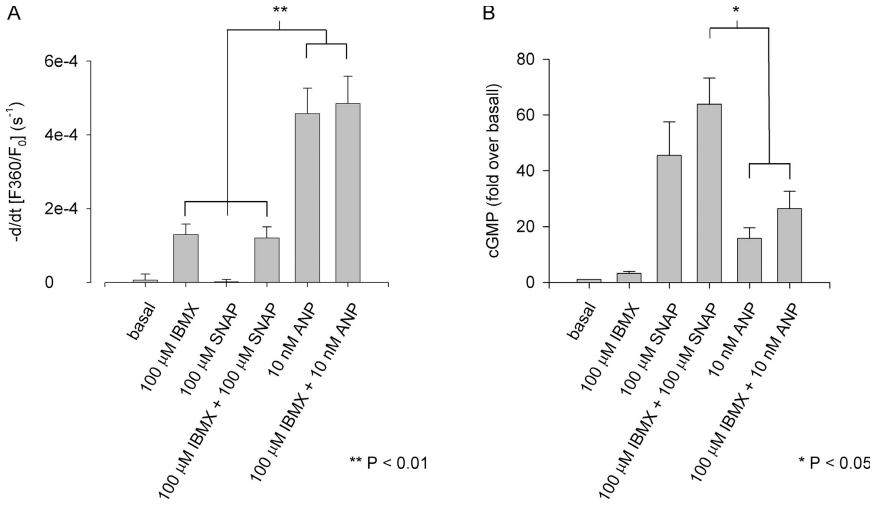

Figure 9. Compartmentalization of cGMP signals in cultured VSMCs. Data were analyzed as described in the text and the legend of Fig. 7. (A) Average of linear fits to the slopes of the fluorescent quench ($n = 4$). The data clearly show that 100 μM SNAP did not significantly activate CNG channels, even in the presence of 100 μM IBMX. Conversely, 10 nM ANP triggered activation of the channels either in the absence or presence of IBMX. (B) Total cGMP levels measured in the same cells using enzyme immunoassays. Treatment of VSMCs with 100 μM IBMX triggered only small increases in cGMP levels. 100 μM SNAP triggered substantial increases in cGMP. In the presence of 100 μM IBMX, 100 μM SNAP triggered the accumulation of significantly more total cGMP than 10 nM ANP ($P < 0.05$). These data indicate that cGMP accumulation triggered by ANP is far more effective in activating CNG channels than the cGMP accumulation triggered by SNAP, even in the presence of 100 μM IBMX. * indicates $P < 0.05$; ** indicates $P < 0.01$.

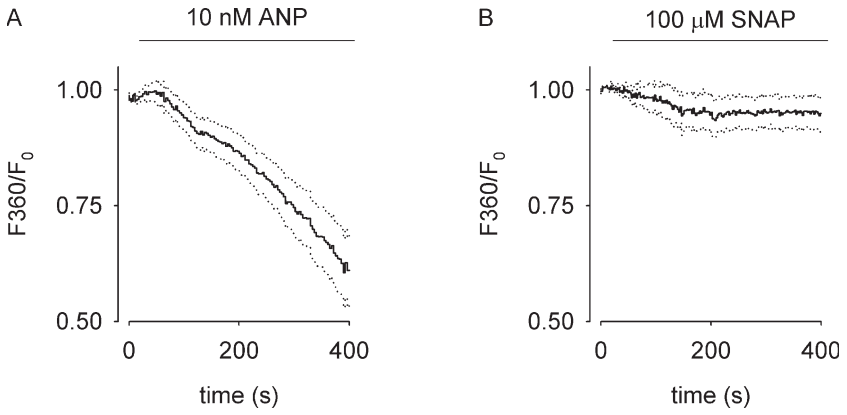

Figure 10. CNG channel activation monitored in single VSMCs. Mn^{2+} influx through CNG channels was monitored in single cells as described in Materials and Methods. Average response (solid line) ± SD (dotted lines) of VSMCs in response to 10 nM ANP (A, $n = 9$) or 100 μM SNAP (B, $n = 14$). Cells exposed to SNAP were subsequently exposed to 10 nM ANP to confirm CNG channel expression. The data indicate that CNG channels expressed in VSMCs respond more readily to 10 nM ANP than to 100 μM SNAP, even though exposure to 100 μM SNAP triggers more cGMP accumulation in these cells. Little or no response was observed in control cells ($n = 12$, not depicted).

within the same subcellular compartments. Although the composition of these compartments is not known, recent studies provided evidence indicating that native olfactory CNG channels and heterologously expressed CNGA2 subunits associate with lipid rafts, but not preferentially with caveolae (Brady et al., 2004). In addition, earlier studies suggest that the particulate guanylyl cyclase NPRB localizes to caveolar membranes (Doyle et al., 1997), and that ANP can be found in the caveolae of atrial myocytes (Page et al., 1994). There is also evidence in freshly dissected aortic rings from rats that indicates sGC localizes to caveolae (Linder et al., 2005). Several lines of evidence also suggest that elements of G protein signaling pathways, including adenylyl cyclase, are associated with lipid rafts, and that localization of these proteins within the plasma membrane is critical for cellular signaling (Huang et al., 1997; Ostrom et al., 2002; Smith et al., 2002). Based upon these studies it is interesting to speculate that lipid rafts help to form discrete subcellular signaling compartments within cells. However, much work is needed to determine if both CNG channels and particulate guanylyl cyclase traffic to the same lipid raft microdomains.

A major challenge in cell biology is understanding how diffusible messengers trigger specific downstream effects. In the absence of mechanisms that slow apparent diffusion rates, both cAMP and cGMP would spread across typical cells in less than a second and compartmentalization could not occur over tens of seconds or minutes (Rich et al., 2000). However, in the last thirty years several groups have observed that increases in cyclic nucleotide concentration do not trigger regulation of all cyclic nucleotide-dependent processes within cells. For example, agents that activate β-adrenergic receptors trigger cAMP-dependent regulation of the contractile machinery in cardiac myocytes, whereas other agents that trigger similar increases in total cAMP levels do not (Brunton et al., 1981; Vila Petroff et al., 2001). Similarly, recent studies have demonstrated that cGMP produced by particulate guanylyl cyclase preferentially regulates plasma membrane–localized targets such as ion channels and pumps, in what is likely a PKG-dependent manner (Zolle et al., 2000; Rho et al., 2002; Zhang et al., 2005a). Our results substantiate the hypothesis that cGMP signaling is compartmentalized in cells, and further suggest that PDE activity alone may not be responsible for the segregation of cGMP signals. An understanding of the mechanisms underlying cGMP compartmentalization is essential because cGMP signaling plays critical roles in both physiological and disease processes. For example, it is unclear why heart failure patients display blunted forearm vasodilation in response to natriuretic peptides, but not in response to NO donors such as nitroprusside (Nakamura et al., 1998). The use of CNG channel-based sensors (Trivedi and Kramer, 1998; Rich et al., 2000, 2001a,b; Trivedi and Kramer, 2002) and recently developed fluorescent sensors (Honda et al., 2001; Mongillo et al., 2004; Ponsioen et al., 2004), in conjunction with ultrastructural, biochemical, and pharmacological approaches, will help to unravel the mechanisms responsible for spatially segregated intracellular signals.

We would like to thank Dr. Chinkers (University of South Alabama College of Medicine, Mobile, AL) for providing HEK-NPRA cells, Drs. Dessauer and Frost for thoughtful discussions about this work, and Drs. Karpen, O'Neil, and Stevens for comments on the manuscript.

This work was supported by National Institutes of Health grants DK59550 (A.P. Morris) and HL074278 (T.C. Rich) and American Heart Association grant 0335084N (T.C. Rich).

Lawrence G. Palmer served as editor.

Submitted: 13 September 2005
Accepted: 23 May 2006

REFERENCES

Abi-Gerges, N., G. Szabo, A.S. Otero, R. Fischmeister, and P.F. Mery. 2002. NO donors potentiate the β-adrenergic stimulation of $I_{Ca,L}$ and the muscarinic activation of $I_{K,ACh}$ in rat cardiac myocytes. *J. Physiol.* 540:411–424.

Airhart, N., Y.F. Yang, C.T. Roberts, and M. Silberbach. 2003. Atrial natriuretic peptide induces natriuretic peptide receptor-cGMP-dependent protein kinase interaction. *J. Biol. Chem.* 278: 38693–38698.

Arnon, A., J.M. Hamlyn, and M.P. Blaustein. 2000. Ouabain augments Ca^{2+} transients in arterial smooth muscle without raising cytosolic Na^{+}. *Am. J. Physiol. Heart Circ. Physiol.* 279:H679–H691.

Baxter, G.F. 2004. Natriuretic peptides and myocardial ischaemia. *Basic Res. Cardiol.* 99:90–93.

Beavo, J.A. 1995. Cyclic nucleotide phosphodiesterases: functional implications of multiple isoforms. *Physiol. Rev.* 75:725–748.

Beavo, J.A., P.J. Bechtel, and E.G. Krebs. 1974. Activation of protein kinase by physiological concentrations of cyclic AMP. *Proc. Natl. Acad. Sci. USA.* 71:3580–3583.

Brady, J.D., T.C. Rich, X. Le, K. Stafford, L. Lynch, J.W. Karpen, R.L. Brown, and J.R. Martens. 2004. Functional role of lipid rafts in cyclic nucleotide-gated channel activation. *Mol. Pharmacol.* 65:503–511.

Bridge, J.H., J.R. Smolley, and K.W. Spitzer. 1990. The relationship between charge movements associated with I_{Ca} and $I_{Na\text{-}Ca}$ in cardiac myocytes. *Science.* 248:376–378.

Broillet, M.-C. 2000. A single intracellular cysteine residue is responsible for the activation of the olfactory cyclic nucleotide-gated channel by NO. *J. Biol. Chem.* 275:15135–15141.

Brunton, L.L., J.S. Hayes, and S.E. Mayer. 1981. Functional compartmentation of cAMP and protein kinase in heart. *Adv. Cyclic Nucleotide Res.* 14:391–397.

Costa, A.D.T., K.D. Garlid, I.C. West, T.M. Lincoln, J.M. Downey, M.V. Cohen, and S.D. Critz. 2005. Protein kinase G transmits the cardioprotective signal from cytosol to mitochondria. *Circ. Res.* In press.

D'Souza, S.P., M. Davis, and G.F. Baxter. 2004. Autocrine and paracrine actions of natriuretic peptides in the heart. *Pharmacol. Ther.* 101:113–129.

Dhallan, R.S., K.-W. Yau, K.A. Schrader, and R.R. Reed. 1990. Primary structure and functional expression of a cyclic nucleotide-activated channel from olfactory neurons. *Nature.* 347:184–187.

Doyle, D.D., S.K. Ambler, J. Upshaw-Earley, A. Bastawrous, G.E. Goings, and E. Page. 1997. Type B atrial natriuretic peptide receptor in cardiac myocyte caveolae. *Circ. Res.* 81:86–91.

Fagan, K.A., T.C. Rich, S. Tolman, J. Schaack, J.W. Karpen, and D.M.F. Cooper. 1999. Adenovirus-mediated expression of an olfactory cyclic nucleotide-gated channel regulates the endogenous Ca^{2+}-inhibitable adenylyl cyclase in C6-2B glioma cells. *J. Biol. Chem.* 274:12445–12453.

Frings, S., R. Seifert, M. Godde, and U.B. Kaupp. 1995. Profoundly different calcium permeation and blockage determine the specific function of distinct cyclic nucleotide-gated channels. *Neuron.* 15:169–179.

Furchgott, R.F., and P.M. Vanhoutte. 1989. Endothelium-derived relaxing and contracting factors. *FASEB J.* 3:2007–2018.

Giordano, D., M. Giorgi, C. Sette, S. Biagioni, and G. Augusti-Tocco. 1999. cAMP-dependent induction of PDE5 expression in murine neuroblastoma cell differentiation. *FEBS Lett.* 446:218–222.

Gray, P.C., J.D. Scott, and W.A. Catterall. 1998. Regulation of ion channels by cAMP-dependent protein kinase and A-kinase anchoring proteins. *Curr. Opin. Neurobiol.* 8:330–334.

Hanafy, K.A., J.S. Krumenacker, and F. Murad. 2001. NO, nitrotyrosine, and cyclic GMP in signal transduction. *Med. Sci. Monit.* 7:801–819.

Hartzell, H.C., and R. Fischmeister. 1986. Opposite effects of cyclic GMP and cyclic AMP on Ca^{2+} current in single heart cells. *Nature.* 323:273–275.

Honda, A., S.R. Adams, C.L. Sawyer, V. Lev-Ram, R.Y. Tsien, and W.R. Dostmann. 2001. Spatiotemporal dynamics of guanosine 3′,5′-cyclic monophosphate revealed by a genetically encoded, fluorescent indicator. *Proc. Natl. Acad. Sci. USA.* 98:2437–2442.

Huang, C., J.R. Hepler, L.T. Chen, A.G. Gilman, R.G.W. Anderson, and S.M. Mumby. 1997. Organization of G proteins and adenylyl cyclase at the plasma membrane. *Mol. Biol. Cell.* 8:2365–2378.

Ignarro, L.J., G. Cirino, A. Casini, and C. Napoli. 1999. Nitric oxide as a signaling molecule in the vascular system: an overview. *J. Cardiovasc. Pharmacol.* 34:879–886.

Kotera, J., K. Fujishige, Y. Imai, E. Kawai, H. Michibata, H. Akatsuka, N. Yanaka, and K. Omori. 1999. Genomic origin and transcriptional regulation of two variants of cGMP-binding cGMP-specific phosphodiesterases. *Eur. J. Biochem.* 262:866–873.

Kotera, J., K.A. Grimes, J.D. Corbin, and S.H. Francis. 2003. cGMP-dependent protein kinase protects cGMP from hydrolysis by phosphodiesterase-5. *Biochem. J.* 372:419–426.

Kuhn, M. 2004. Molecular physiology of natriuretic peptide signalling. *Basic Res. Cardiol.* 99:76–82.

Kwan, C.Y., and J.W. Putney. 1990. Uptake and intracellular sequestration of divalent cations in resting and methacholine-stimulated mouse lacrimal acinar cells. Dissociation by Sr^{2+} and Ba^{2+} of agonist-stimulated divalent cation entry from the refilling of the agonist-sensitive intracellular pool. *J. Biol. Chem.* 265:678–684.

Leblanc, N., and J.R. Hume. 1990. Sodium current-induced release of calcium from cardiac sarcoplasmic reticulum. *Science.* 248:372–376.

Lederer, W.J., E. Niggli, and R.W. Hadley. 1990. Sodium-calcium exchange in excitable cells: fuzzy space. *Science.* 248:283.

Li, H., J.P. Liu, and P.J. Robinson. 1996. Multiple substrates for cGMP-dependent protein kinase from bovine aortic smooth muscle: purification of P132. *J. Vasc. Res.* 33:99–110.

Lin, C.S., S. Chow, A. Lau, R. Tu, and T.F. Lue. 2001. Regulation of human PDE5A2 intronic promoter by cAMP and cGMP: identification of a critical Sp1-binding site. *Biochem. Biophys. Res. Commun.* 280:693–699.

Linder, A.E., L.P. McCluskey, K.R. Cole, K.M. Lanning, and R.C. Webb. 2005. Dynamic association of nitric oxide downstream signaling molecules with endothelial caveolin-1 in rat aorta. *J. Pharmacol. Exp. Ther.* 314:9–15.

Martin, A.R., and P.A. Fuchs. 1992. The dependence of calcium-activated potassium currents on membrane potential. *Proc. Biol. Sci.* 250:71–76.

Martins, T.J., M.C. Mumby, and J.A. Beavo. 1982. Purification and characterization of a cyclic GMP-stimulated cyclic nucleotide phosphodiesterase from bovine tissues. *J. Biol. Chem.* 257:1973–1979.

Mongillo, M., T. McSorley, S. Evellin, A. Sood, V. Lissandron, A. Terrin, E. Huston, A. Hannawacker, M.J. Lohse, T. Pozzan, et al. 2004. Fluorescence resonance energy transfer-based analysis of cAMP dynamics in live neonatal rat cardiac myocytes reveals distinct functions of compartmentalized phosphodiesterases. *Circ. Res.* 95:67–75.

Nakamura, M., N. Arakawa, H. Yoshida, S. Makita, H. Niinuma, and K. Hiramori. 1998. Vasodilatory effects of B-type natriuretic peptide are impaired in patients with chronic heart failure. *Am. Heart J.* 135:414–420.

Ostrom, R.S., X. Liu, B.P. Head, C. Gregorian, T.M. Seasholtz, and P.A. Insel. 2002. Localization of adenylyl cyclase isoforms and G protein-coupled receptors in vascular smooth muscle cells: expression in caveolin-rich and noncaveolin domains. *Mol. Pharmacol.* 62:983–992.

Page, E., J. Upshaw-Earley, and G.E. Goings. 1994. Localization of atrial natriuretic peptide in caveolae of in situ atrial myocytes. *Circ. Res.* 75:949–954.

Palmer, D., and D.H. Maurice. 2000. Dual expression and differential regulation of phosphodiesterase 3A and phosphodiesterase 3B in human vascular smooth muscle: implications for phosphodiesterase 3 inhibition in human cardiovascular tissues. *Mol. Pharmacol.* 58:247–252.

Ponsioen, B., J. Zhao, J. Riedl, F. Zwartkruis, G. van der Krogt, M. Zaccolo, W.H. Moolenaar, J.L. Bos, and K. Jalink. 2004. Detecting cAMP-induced Epac activation by fluorescence resonance

energy transfer: Epac as a novel cAMP indicator. *EMBO Rep.* 5:1176–1180.

Potter, L.R., S. Abbey-Hosch, and D.M. Dickey. 2005. Natriuretic peptides, their receptors and cGMP-dependent signaling functions. *Endocr. Rev.* In press.

Rho, E.H., W.J. Perkins, R.R. Lorenz, D.O. Warner, and K.A. Jones. 2002. Differential effects of soluble and particulate guanylyl cyclase on Ca^{2+} sensitivity in airway smooth muscle. *J. Appl. Physiol.* 92:257–263.

Rich, T.C., and J.W. Karpen. 2002. Cyclic AMP sensors in living cells: what signals can they actually measure? *Ann. Biomed. Eng.* 30:1088–1099.

Rich, T.C., and J.W. Karpen. 2005. High-throughput screening of PDE activity in living cells. *Methods Mol. Biol.* 307:45–62.

Rich, T.C., K.A. Fagan, H. Nakata, J. Schaack, D.M.F. Cooper, and J.W. Karpen. 2000. Cyclic nucleotide-gated channels colocalize with adenylyl cyclase in regions of restricted cAMP diffusion. *J. Gen. Physiol.* 116:147–161.

Rich, T.C., K.A. Fagan, T.E. Tse, J. Schaack, D.M.F. Cooper, and J.W. Karpen. 2001a. A uniform extracellular stimulus triggers distinct cAMP signals in different compartments of a simple cell. *Proc. Natl. Acad. Sci. USA.* 98:13049–13054.

Rich, T.C., T.E. Tse, J.G. Rohan, J. Schaack, and J.W. Karpen. 2001b. In vivo assessment of local phosphodiesterase activity using tailored cyclic nucleotide-gated channels as cAMP sensors. *J. Gen. Physiol.* 118:63–77.

Ruskoaho, H., R.E. Lang, M. Toth, D. Ganten, and T. Unger. 1987. Release and regulation of atrial natriuretic peptide (ANP). *Eur. Heart J.* 8 (Suppl. B):99–109.

Rybalkin, S.D., C. Yan, K.E. Bornfeldt, and J.A. Beavo. 2003. Cyclic GMP phosphodiesterases and regulation of smooth muscle function. *Circ. Res.* 93:280–291.

Schulz, S., M. Chinkers, and D.L. Garbers. 1989. The guanylate cyclase/receptor family of proteins. *FASEB J.* 3:2026–2035.

Smith, K.E., C. Gu, K.A. Fagan, B. Hu, and D.M.F. Cooper. 2002. Residence of adenylyl cyclase type 8 in caveolae is necessary but not sufficient for regulation by capacitative Ca^{2+} entry. *J. Biol. Chem.* 277:6025–6031.

Soderling, S.H., S.J. Bayuga, and J.A. Beavo. 1998. Identification and characterization of a novel family of cyclic nucleotide phosphodiesterases. *J. Biol. Chem.* 273:15553–15558.

Trivedi, B., and R.H. Kramer. 1998. Real-time patch-cram detection of intracellular cGMP reveals long-term suppression of responses to NO and muscarinic agonists. *Neuron.* 21:895–906.

Trivedi, B., and R.H. Kramer. 2002. Patch cramming reveals the mechanism of long-term suppression of cyclic nucleotides in intact neurons. *J. Neurosci.* 22:8819–8826.

Vila Petroff, M.G., J.M. Egan, X. Wang, and S.J. Sollott. 2001. Glucagon-like peptide-1 increases cAMP but fails to augment contraction in adult rat cardiac myocytes. *Circ. Res.* 89:445–452.

Waldman, S.A., and F. Murad. 1988. Biochemical mechanisms underlying vascular smooth muscle relaxation: the guanylate cyclase-cyclic GMP system. *J. Cardiovasc. Pharmacol.* 12(Suppl. 5): S115–S118.

Wollert, K.C., S. Yurukova, A. Kilic, F. Begrow, B. Fiedler, S. Gambaryan, U. Walter, S.M. Lohmann, and M. Kuhn. 2003. Increased effects of C-type natriuretic peptide on contractility and calcium regulation in murine hearts overexpressing cyclic GMP-dependent protein kinase I. *Br. J. Pharmacol.* 140:1227–1236.

Wyatt, T.A., A.J. Naftilan, S.H. Francis, and J.D. Corbin. 1998. ANF elicits phosphorylation of the cGMP phosphodiesterase in vascular smooth muscle cells. *Am. J. Physiol.* 274:H448–H455.

Zhang, Q., J. Moalem, J. Tse, P.M. Scholz, and H.R. Weiss. 2005a. Effects of natriuretic peptides on ventricular myocyte contraction and role of cyclic GMP signaling. *Eur. J. Pharmacol.* 510:209–215.

Zhang, Q., P.M. Scholz, Y. He, J. Tse, and H.R. Weiss. 2005b. Cyclic GMP signaling and regulation of SERCA activity during cardiac myocyte contraction. *Cell Calcium.* 37:259–266.

Zhang, S., Y. Yang, B.C. Kone, J.C. Allen, and A.M. Khan. 2003. Insulin-stimulated cyclic guanosine monophosphate inhibits vascular smooth muscle cell migration by inhibiting Ca/calmodulin-dependent protein kinase II. *Circulation.* 107:1539–1544.

Zolle, O., A.M. Lawrie, and A.W.M. Simpson. 2000. Activation of the particulate and not the soluble guanylate cyclase leads to the inhibition of Ca^{2+} extrusion through localized elevation of cGMP. *J. Biol. Chem.* 275:25892–25899.